Remote Sensing of the Nearshore

Rob Holman[1] and Merrick C. Haller[2]

[1]College of Earth, Ocean, and Atmospheric Sciences and [2]School of Civil and Construction Engineering, Oregon State University, Corvallis, Oregon 97331;
email: holman@coas.oregonstate.edu, merrick.haller@oregonstate.edu

Annu. Rev. Mar. Sci. 2013. 5:95–113

First published online as a Review in Advance on July 23, 2012

The *Annual Review of Marine Science* is online at marine.annualreviews.org

This article's doi:
10.1146/annurev-marine-121211-172408

Keywords

littoral, electro-optical, microwave, marine radar, bathymetry, infrared

Abstract

The shallow waters of the nearshore ocean are popular, dynamic, and often hostile. Prediction in this domain is usually limited less by our understanding of the physics or by the power of our models than by the availability of input data, such as bathymetry and wave conditions. It is a challenge for traditional in situ instruments to provide these inputs with the appropriate temporal or spatial density or at reasonable logistical or financial costs. Remote sensing provides an attractive alternative. We discuss the range of different sensors that are available and the differing physical manifestations of their interactions with the ocean surface. We then present existing algorithms by which the most important geophysical variables can be estimated from remote sensing measurements. Future directions and opportunities will depend on expected developments in sensors and platforms and on improving processing algorithms, including data assimilation formalisms.

1. INTRODUCTION

The nearshore is the narrow strip of the ocean that borders the continents. It can be dynamically defined as the coastal region that is significantly affected by surface gravity waves, so it spans from the farthest inland reach of storm waves to offshore depths of $O(10\ \text{m})$, beyond which bathymetric change is no longer due to wave motions. Although the nearshore represents only 10^{-3} of the ocean's surface area and 10^{-6} of its volume, it is the part that is best known and dearest to humans and is a critical resource for recreation, industry, ecosystem services, commerce, and defense.

Despite its proximity to civilization, the nearshore can be a difficult domain to sample and understand. Breaking waves in the surf zone are often violent and wave-driven currents can be strong, which makes work in the surf zone dangerous to both people and instruments. Because sandy bottoms can undergo substantial erosion or accretion over surprisingly short periods, traditional bottom-mounted sensors are often rapidly scoured out or buried. Water-level changes due to the tide can be large, changing a fixed sensor's domain from being too deep to be interesting at high tide to high and dry at low tide.

These harsh and challenging conditions make long-duration in situ observations in the surf zone problematic but suggest the potential benefits of remote sensing approaches. Although most people associate remote sensing with satellites, a number of other solutions are available, from airborne sensors on manned and unmanned platforms to shore-based sensors mounted on lighthouses, towers, and bluffs. All have the advantage that sensors can be installed away from harsh marine conditions; can often have direct access to the power grid, storage, and the Internet; and can usually observe a large spatial extent over long durations at a lower cost.

This review discusses the various aspects of the fairly new discipline of nearshore remote sensing. This type of remote sensing is a specific example of the recent growth of ocean observing technologies, but the particular requirements of nearshore sampling have led to solutions different from those used in those programs, and the approaches have had more time to mature.

The nearshore has been sampled by a full suite of both active and passive remote sensors (cameras, radars, lidars, etc.) using a range of platforms (fixed, flying, floating, and orbiting) and operating across the visible, infrared (IR), microwave, and radio bands of the electromagnetic (EM) spectrum. However, for nearshore oceanographic applications, fixed optical cameras and X-band radars are the most frequently used and best developed, and so these are the main focus of the discussion of retrieval algorithms in Section 3.

In Section 1.1, we discuss some aspects of the nearshore domain to constrain the requirements of an ideal sampling system. In Section 1.2 we describe some specific challenges faced when using remote sensors. This is followed in Section 2 by a discussion of platforms and sensors and their respective exploitable signatures. Section 3 provides examples of operational systems and algorithms that have been developed to extract geophysical signals from remotely sensed data. We finish in Section 4 with potential future developments in nearshore observing packages that merge multiple sensor inputs with numerical models to yield a full characterization of the nearshore domain.

1.1. Requirements of a Nearshore Sampling System

The dynamics of the nearshore are driven primarily by ocean wave energy that has been generated elsewhere and propagated into the nearshore domain. Unlike the deeper ocean, where local winds cause oversteepening, the dissipation of nearshore energy is due to depth limitation and occurs in a narrow strip, commonly only 100 m wide, with typical rates of 10–100 W m^{-2}—one of the strongest signals in oceanography. These processes, in turn, drive nearshore currents and

circulation as well as the sediment transport that creates nearshore sand bars and complex bottom morphology.

The goal of nearshore science is to understand, characterize, and predict the evolving waves, currents, and bathymetry over any nearshore region for which observations are available. Solutions have inevitably consisted of core numerical models, which have shown increasing skill when fed with accurate bathymetry and offshore wave data (e.g., see Ruessink et al. 2001), along with the methods to provide that required input data. For all but a few well-instrumented field sites, prediction accuracy is limited by data availability, particularly for bathymetry data, the gathering of which usually requires expensive sampling methods and can be done only occasionally. Thus, data assimilation methods must be used to merge available observations with models to yield dynamically consistent estimates of flow variables and bathymetry (e.g., see Wilson et al. 2010).

The requirements for successful sampling of the nearshore are governed by the time and space scales of variability within the system. Visually, the most obvious timescale is associated with the O(10 s) periods of surface waves. However, the nearshore spectrum often includes significant motions at longer scales such as infragravity waves (30–300-s periods) driven by wave groups (Herbers et al. 1995), very low-frequency motions (10^2–10^3-s periods) arising from current instabilities (Oltman-Shay et al. 1989), and longer timescales associated with system modulation by tides (Thornton & Kim 1993), not to mention episodic extreme events such as storms and hurricanes. Sand bars and bottom profile shapes evolve on timescales as short as days and force corresponding changes in the hydrodynamics. The 1–10-Hz sampling capability of most existing in situ sensors is adequate for high-frequency needs, but the requirement for extended sampling under difficult conditions usually leads to sensor degradation and excessive expense.

In the spatial domain, the nearshore is a region of high inhomogeneity. Surf zone motions and morphology are rarely uniform alongshore and so must also be sampled in the alongshore direction. Wave-breaking processes, in turn, drive nearshore currents with similar spatial variability and induce the sediment transport that creates nearshore sand bars, complex bottom morphologies, and eroding or accreting beaches.

Wave motions, currents, and bathymetry all vary strongly over 10–1,000-m cross-shore scales. Proper sampling of this wide range of spatial scales would require a large array of in situ point sensors. In contrast, most remote sensors operate in an imaging mode that is optimized for such spatial sampling needs. However, the need for spatial sampling often competes with requirements for the rate and duration (dwell) of temporal sampling. For example, moving remote sensing platforms (e.g., airplanes) maximize their spatial sampling capability at the expense of dwell.

1.2. Issues Specific to Remote Sensing

Several issues complicate the use of remote sensing data. For example, passive sensors such as cameras and radiometers operate by capturing photons that are reflected and/or emitted from the ocean surface. An array of receivers (pixels) are then combined to form an image. However, in contrast to data collected by most in situ sensors, the geolocation of features seen within these images is not unique, because pixels correspond to unique look directions but not unique distances. Reasonable assumptions can often be made that allow full solutions using standard photogrammetric methods; for example, the vertical location of the ocean surface can be effectively treated as residing at sea level (e.g., see Holland et al. 1997). This problem is much reduced for active sensors, where distances are determined from the time of flight between the transmitted and received pulses and azimuths from the sensor viewing geometry. However, for any moving platform, the accurate measurement of platform motion and viewing geometry creates additional challenges.

Figure 1

Optical snapshot of nearshore waves at Duck, North Carolina. Although a casual observer easily picks out the longer incident waves, variability is dominated by short chop that must be accounted for in processing algorithms.

More difficult than the mapping issue is the problem of quantifying the relationship between remotely sensed signals and the geophysical variables that we wish to measure, usually referred to as a retrieval algorithm and the subject of much of the research (Section 3). In some cases, relationships have already been established—for example, the relationship between optical reflectivity and sea surface slope for unbroken ocean waves based on Maxwell's equations (Walker 1994) or that between microwave backscatter and sea surface characteristics under mild winds described by composite surface theory (Valenzuela 1968, Wright 1968). In other cases, retrieved estimates serve as inputs for the indirect estimation of other variables, such as wave energy from measurements of sea surface slope or water depth from measurements of ocean wave periods and lengths (Section 3).

Remote sensors often have the opposite problem of data starvation, i.e., too much data. For example, a single video camera can easily deliver 35 MB s^{-1}, and five cameras are commonly needed to span the full 180° field of view. Twelve hours of daylight would then yield 7.2 TB, a proverbial fire hose of data that is difficult to even return from a remote site, let alone analyze. Fortunately, for nearshore applications the full sampling capability of video cameras is not required and can therefore be downscaled to approximately 2-Hz sampling at a 5-m spatial resolution. This represents a 10,000-fold reduction in the data rate, enabling finite logistics to be stretched for longer dwell and larger spatial coverage (footprint).

Finally, remote sensing data are often surprisingly noisy—see, for example, the optical image shown as **Figure 1**. Although a casual observer sees the longer incident waves, the above-mentioned sea surface slope dependence means that short-wave clutter dominates the image data and must be appropriately dealt with in any retrieval algorithm. The presence of fog, low wind, or rain also contributes to data degradation. To bound this problem, retrieval algorithms must include corresponding confidence estimates. Recent developments in data assimilation have yielded mature approaches by which observations of varying quality and believability can be incorporated into modeling frameworks, provided that confidence estimates are available (Feddersen et al. 2004, Kurapov et al. 2007, Wilson et al. 2010).

2. PLATFORMS, SENSORS, AND SIGNATURES

2.1. Platforms

Sensors can be mounted at fixed locations or on ships, planes, or satellites. Each platform has advantages and trade-offs, particularly between dwell and footprint. Sensors at fixed locations, such as cameras in a lighthouse or on a tall building, can have unlimited dwell and have a fixed viewing geometry such that the relationship between image and world location is fixed and need only be solved once (Holman & Stanley 2007; note, however, that the viewing angles of even fixed cameras change slightly owing to thermal or wind stresses, a potential issue if high accuracy is needed). As a general rule, the prime advantage provided by all remote sensors is their large footprint compared with in situ instruments.

Although fixed platforms have the advantage of allowing essentially unlimited dwell, many locations lack the high vantage point needed for sampling in the optical and IR bands (both wave shadowing and range resolution degrade as tilts approach the horizon) or are only of occasional interest and not deemed worthy of the investment in a fixed station. Others may be of military interest and denied to fixed platforms. For these locations, sampling from moving platforms becomes an attractive alternative. Satellite sensing is well known (for a review of coastal system applications, see Klemas 2011), has global coverage, is commonly supported by national or international agency funding, and has a mature set of support infrastructures and software. However, satellites are a limited resource, have limited or no dwell capability, and are tasked only through a necessarily very restrictive process. Airborne sensors allow much easier access and control, and a wide range of platforms are becoming available (e.g., Irish & Lillycrop 1999, Dugan et al. 2001b). Manned aircraft remain moderately expensive because they are usually below the threshold costs for national system support, so the costs are borne directly by investigators. However, there has been an increasing proliferation of unmanned aerial vehicles (UAVs), ranging from large military vehicles to surprisingly useful hobby-level systems. The maturity of analysis and support software for airborne data usually lags behind that for satellites, but flexibility increases correspondingly.

Although spatial coverage is good for overhead moving sensors, many retrieval algorithms exploit time-dependent signatures and so require sampling at relevant timescales (seconds for waves) over a useful dwell (perhaps minutes). Such data are not available from satellites and require special operations for airborne systems such as making a slow helicopter flight, "staring" using a gimbaled camera in spotlight mode (Dugan et al. 2001a), or flying in an appropriate pattern such that a camera rigidly attached to the airframe remains pointed at some geographic location. Dwell requirements depend on the retrieval algorithm (Section 3).

With the need for dwell on moving platforms come the associated problems of the time-varying geolocation of each image. In principle this is just an inconvenience due to increased bookkeeping, because sensor position and viewing angle data are usually recorded continuously—see, for example, the analysis of radar data from a moving ship by Bell & Osler (2011). However, accuracy requirements, particularly for viewing angles, can be daunting. A 1° gyro error for a 1,000-m-altitude, obliquely viewing camera yields a 35-m ground error, which is roughly a full ocean wavelength in the nearshore. Very good gyros can be purchased, but often come at great expense and with a weight beyond the payload or power capacity of many small UAVs. Typically, airborne imagery must be stabilized (i.e., rectified using imaged ground-control points) in postprocessing to be useful. Stabilization methods for scenes that include only water and moving waves do not yet exist, so images must include some fraction of land coverage.

Finally, the physics by which waves are seen by sensors usually depends on the viewing angles. For example, because optical and IR sensors see wave contrast due to variations in sea surface slope

in the look direction, contrast is much greater when viewing into an oncoming wave field than when viewing across it (which explains why wave direction appears to be different looking forward than it does looking backward from a window when flying in airplanes). Thus, the transfer function between observables and geophysical quantities is variable for sensors on moving platforms in ways that must be accounted for.

2.2. Available Sensors

All remote sensors measure the strength of EM radiation coming from an observed scene. Active sensors, such as radars and lidars, act as both the source and detector of this energy, whereas passive sensors, such as optical and IR cameras, rely on ambient sources of illumination. This radiation interacts with the sea surface according to Maxwell's equations, but the manifestations for the different sensors vary considerably because of their very different EM wavelengths.

The visible band used by optical sensors—commonly referred to as electro-optical (EO)—spans wavelengths from 400 (violet) to 700 (red) nm. When light hits the dielectric surface of the ocean, part is reflected and the remainder is transmitted into the interior, where it can attenuate or scatter from water molecules or particulates, possibly reemerging through the surface as upwelling radiance (Mobley 1994, Walker 1994). The air-water reflection coefficient is only 2% at normal incidence, so near-nadir optical measurements are dominated by the effects of water column characteristics. However, for incidence angles greater than 60° (measured from the vertical), reflection increases rapidly, and optical sensors therefore become primarily ocean surface sensors (this variation is evident in **Figure 1**). It is the variation of incidence angle with the local sea surface slope that provides much of the contrast by which waves become visible (**Figure 1**). The reflection coefficient also depends on the polarity of the incident light: An initially unpolarized source is polarized upon reflection in a manner that can be inverted for wave characteristics (Section 3).

The approximately 700-nm to 300-μm wavelengths of IR energy are much longer than optical wavelengths and include the midrange thermal wavelengths of 3–10 μm that are being studied for nearshore remote sensing applications (Watanabe & Mori 2008). As with optical wavelengths, reflection is very low at small incidence angles and increases rapidly above 60°. However, IR energy attenuates within a few wavelengths in water, so the backscattered contribution to upwelled energy is never observed. Instead, the ocean directly radiates IR energy due to the black body (thermal) radiation that is the dominant source for small to moderate incidence angles. Because evaporation causes the formation of a submillimeter-thick cool skin on the ocean surface, IR sensors often see patchy patterns associated with the disruption of this surface layer by turbulence (Jessup et al. 1997, Siddiqui et al. 2001, Zappa et al. 2004). These features can be used as ephemeral water mass trackers for particle image velocimetry (PIV) analysis (Section 3). In contrast to EO cameras, IR sensors continue to work at night, although the signature physics differ between day and night.

The term radar describes active sensors that operate anywhere across a broad region of the microwave and radio portions of the EM spectrum, typically at wavelengths between 1 cm and 100 m. Marine radars operate at both S- and X-band wavelengths, but the 3-cm wavelength and 5–10-m spatial resolution of X-band microwave radiation are most appropriate to nearshore remote sensing. In contrast to imaging cameras, the rotating antenna of a radar builds an image with pixels captured in a serial fashion. Pulses transmitted at approximately 2,000 Hz intersect the ocean surface along a radial that is approximately 1°–3° wide in azimuth, and the returning echoes are recorded as a function of time of flight, and hence range, out to 1–3 km (for a review, see Gommenginger et al. 2000). Because marine radars typically spin at a rate of 25–45 rotations per minute, the ocean scene is not captured synoptically but rather takes $O(1\ s)$ to be constructed,

a duration that is significant for some analyses but still an order of magnitude faster than typical ocean wave periods. (We do not discuss high-frequency radars with 10–100-m wavelengths here because they sample with a resolution that is too coarse for nearshore applications.)

Microwave reflection is again strong for the high (near-horizontal) incidence angles typical of shore-based radar scanning. Like IR, any energy that is transmitted into the water column is very rapidly attenuated and not backscattered. Because reflection is strong and incidence angles near grazing, signal return from a smooth sea will be negligible—radar does not see unbroken offshore waves on windless days. Instead, radar returns are the result of surface backscatter from roughness and other surface features that are of similar or smaller size compared with the radar wavelength (and so are not smooth on a radar length scale). Also, because microwave pulses are electrically generated, they are always polarized along either the horizontal or vertical axis, with different reflection and backscattering characteristics for each.

Radars mounted on moving platforms can be processed in a synthetic aperture radar (SAR) mode (Curlander & McDonough 1991) wherein information from radar returns are accumulated over time and processed to yield an image whose spatial resolution is equivalent to that which would be obtained using a radar antenna whose length is the total flight length during sampling. SAR yields high-resolution images of fixed scenes but can produce artifacts of spatial displacement for moving features like ocean waves. These can be reasonably corrected, but only with moderately complex processing.

Because EO, IR, and radar sensors respond to different aspects of the ocean surface and interior, observations that combine multiple sensors are expected to yield more information than the sum of observations from the individual sensors (Branch et al. 2008, Catalan et al. 2011).

3. RETRIEVAL ALGORITHMS

Humans viewing the ocean have access to remarkable subconscious processing algorithms that allow the isolation of features of interest (such as waves) from a large suite of competing noise sources (**Figure 1**). For instruments and sensors, similar processing needs must be manually identified and implemented as part of analysis algorithms. Because these usually rely on some kind of filtering in time or space, data sources must be temporally and/or spatially extensive.

The following algorithm descriptions assume data that are temporally long and spatially extensive compared with the dominant signals (ocean waves). These are typical characteristics of fixed-platform remote sensing data such as those gathered by the Argus program (Holman & Stanley 2007) for nearshore optical remote sensing and equivalent algorithms that have been developed for nearshore marine radar data. It has recently been recognized that, owing to the complementary resolution, range, and footprint characteristics of optical cameras and X-band marine radars, the combined results of these two remote sensors at any site can provide a richer picture of the observed nearshore dynamics (van Dongeren et al. 2008, Perkovic et al. 2009, Catalan et al. 2011).

The goal of retrieval algorithms is to provide estimates and confidence intervals for important nearshore geophysical quantities related to waves, currents, and bathymetry. Specific retrieval algorithms of interest include those applicable to wave directional distributions (e.g., Young et al. 1985, Izquierdo & Soares 2005), wave heights (Borge et al. 1999, Dankert & Rosenthal 2004, de Vries et al. 2011, Almar et al. 2012), the occurrence of wave breaking (Lewis & Olin 1980, Bass & Hay 1997, Haller & Lyzenga 2003), wave dissipation (e.g., Lippmann & Holman 1989, McGregor et al. 1998, Aarninkhof & Ruessink 2004, Haller & Catalan 2009), wave run-up and inundation (e.g., Aagaard & Holm 1989, Walton 1993, Hasan & Takewaka 2009, Bryan & Coco 2010, Rueben et al. 2011), morphology (e.g., Lippmann & Holman 1990, Ruessink et al. 2002,

Clarke & Werner 2003, Alexander & Holman 2004, McNinch 2007, Elsayed & Takewaka 2008), bathymetry (e.g., Bell 1999, Stockdon & Holman 2000, Aarninkhof et al. 2003, Flampouris et al. 2008), and surf zone currents (Chickadel et al. 2003, Puleo et al. 2003, Perkovic et al. 2009). Each algorithm exploits different remote sensing signatures. Algorithms to isolate signals from noise are often based on the assumption that the many processes that contaminate and confuse desired signals can be separated by time or space scales. For example, energetic ocean waves usually have spatial scales that are intermediate between those of short-wave clutter and across-image lighting trends. Scale partitioning is usually done by Fourier analysis. Because retrieval results vary in quality depending on viewing conditions (rain, fog, night) and the nature of the geophysical signal (e.g., glassy calm), results must always be accompanied by objective confidence intervals.

3.1. Wave Characteristics

Wave motions provide the energy that drives currents and circulation as well as the sediment transport by which the bathymetry evolves. Thus, remote sensing estimation of wave conditions provides a necessary input for nearshore numerical models. Wave forcing can be represented in a parametric fashion (a representative wave height, H; period, T; and angle of approach, α) or as a potentially continuous distribution across a range of frequency, f, and wave direction space.

Different sensors image waves through different mechanisms. For unbroken waves, visible- and IR-band sensors principally sense variations in reflection or emission with sea surface slope, a dependence that is strongest for near-horizontal viewing (e.g., **Figure 2**) (for optics, see Walker 1994). Breaking waves are bright in optical images owing to the strong combined backscatter of light weakly reflecting from individual bubble surfaces in a thick foam layer. IR images of bubbles in breaking waves are also bright owing to the high emissivity of thin bubble surfaces, although evaporation overwhelms this signal within seconds and the foam then appears cool (C. Chickadel, personal communication).

Because transmitted radar waves will only reflect back to shore-based sensors in the highly unlikely case of normal incidence (a wave face exactly normal to the sensor), measured returns are dominated by backscatter processes from sea surface roughness that is short compared with the radar wavelength. The most common mechanism is Bragg backscatter, which is caused by roughness with a length scale in the range direction that is exactly half of the radar wavelength (Alpers et al. 1981, Plant 1991), but radar waves also strongly scatter from sharp crests and breaking wave roughness (Fuchs et al. 1999, Coakley et al. 2001, Ja et al. 2001).

Figure 3 is an example marine radar image of (uncalibrated) backscatter strength taken at the mouth of Yaquina Bay in Newport, Oregon. The image shows swell waves approaching from the northwest direction refracting toward the shore normal on the open beach. The processes of shoaling and diffraction can also be seen through the shortening of the wavelengths closer to shore and the curved wave crests in the lee of the southern jetty. In addition to backscatter strength, some radars measure the Doppler shift of reflected pulses from which the range component of water velocity can be found (e.g., Puleo et al. 2003, Perkovic et al. 2009). However, coherent marine radars are not yet commercially available.

Sequences of images of wave phase such as those shown in **Figures 1–3** allow estimation of the frequency, direction, and wavelength characteristics of incident waves (Dugan et al. 2001b; R.A. Holman, N.G. Plant & K.T. Holland, manuscript in review). However, these estimates describe the frequency-directional distribution of some observed variable, such as radar backscatter or optical intensity, rather than the characteristics of a desired geophysical variable, such as sea surface elevation. Transfer functions between observed and desired variables have been proposed and show some skill (e.g., Plant & Keller 1983), but they rely on a number of assumptions and so are only

Figure 2

Daytime infrared snapshot of nearshore waves at Duck, North Carolina. Bright tones are warm. The beach is very warm but the higher swash zone very cool owing to evaporation. The overall cooling with distance corresponds to reducing emissions with increasing incidence angle (toward the horizon). Wave faces are seen offshore owing to their smaller local incidence angles (wave faces are sloped toward the camera). Breaking waves emit strongly and so appear very warm, but residual foam left by the breakers rapidly cools by evaporation and so appears cool. Image courtesy of Chris Chickadel, Applied Physics Laboratory, University of Washington.

approximate. In contrast, the reflection of light by a dielectric ocean surface alters its polarization characteristics in ways that are specified directly by Maxwell's equations and depend only on the cross-look component of sea surface slope, a fundamental geophysical quantity. Although short-wave clutter degrades signal-to-noise ratio and the polarization of incident illumination is often not random, the exploitation of polarimetric optical observations for wave height estimation remains a promising research topic (Zappa et al. 2008).

3.2. Wave Dissipation

Wave dissipation in the nearshore is the attenuation of waves due to depth-limited breaking and occurs when waves reach depths roughly equal to the wave height (Thornton & Guza 1982). The dissipation of incident waves in the surf zone is important for more than just its role in the wave energy budget. Longuet-Higgins & Stewart (1964) demonstrated that ocean surface waves carry with them a momentum flux called radiation stress that is proportional to the wave energy. When this wave energy dissipates, it causes a transfer of that momentum (to force mean flows) that is in direct proportion to the dissipation. Thus, direct measurement of wave dissipation is equivalent to measuring the forcing for nearshore flows. In situ measurements of local wave dissipation are difficult and rare, but breaking waves have strong signatures for all remote sensors, suggesting the potential power of this remote sensing capability.

Several relationships have been proposed between observable quantities and dissipation. Lippmann & Holman (1989) used an existing model for dissipation of a random wave field over

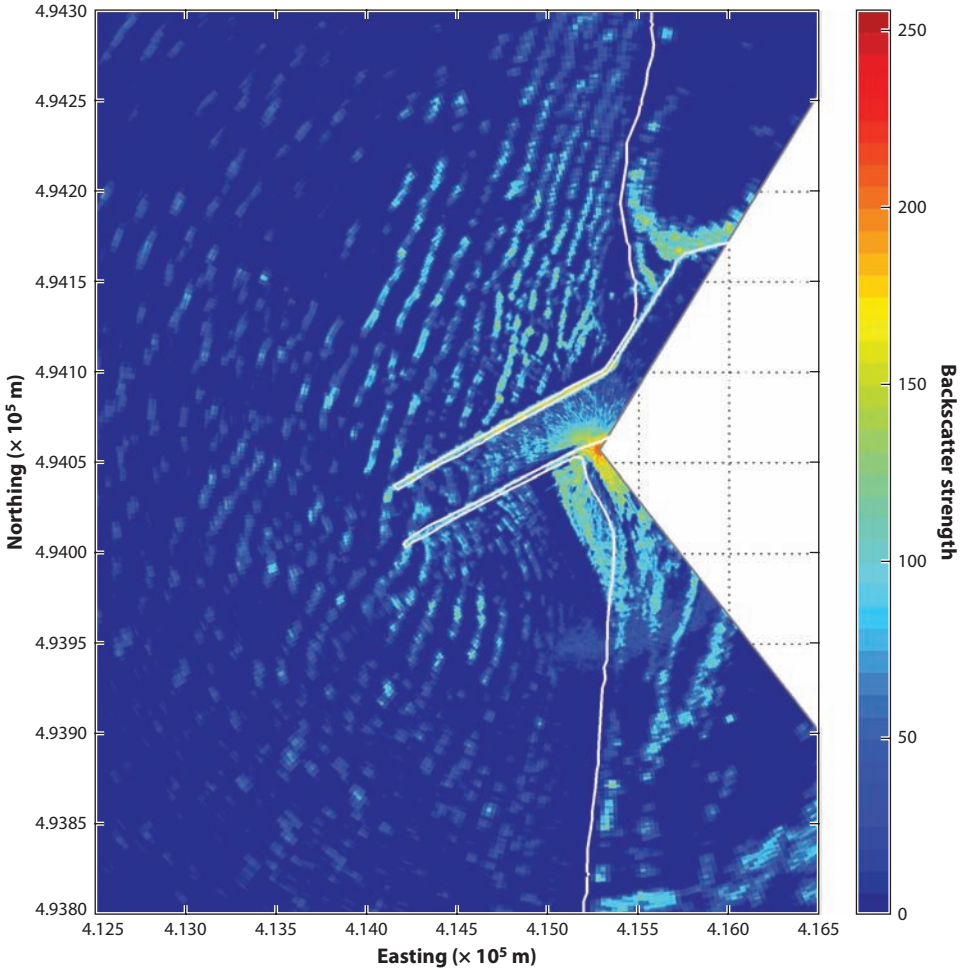

Figure 3

Snapshot radar backscatter image showing waves approaching the shoreline at Yaquina Bay in Newport, Oregon. Yaquina jetties and an approximate shoreline contour are shown in white.

barred topography and showed that the bright white bands seen in time exposure images (e.g., **Figure 4*b***) corresponded well with expected dissipation maxima, and so served as a good proxy for the position of submerged sand bars. However, they did not attempt to make direct estimates of dissipation from the optical signal alone.

Svendsen (1984) first suggested that wave rollers (the white masses of bubbles and foam that surf down the front surface of breaking waves) play a key role in wave dissipation and the resulting forcing of mean flows in the surf zone and, based on physical arguments first posed by Duncan (1981), proposed a relationship between roller dissipation and the volume of the roller. Haller & Catalan (2009) were able to demonstrate that, based on this relationship, optical measurements of the horizontal size of surf zone breakers in the laboratory could then be used to estimate dissipation directly. Catalan et al. (2011) extended this methodology to field observations by using combined optical and radar observations.

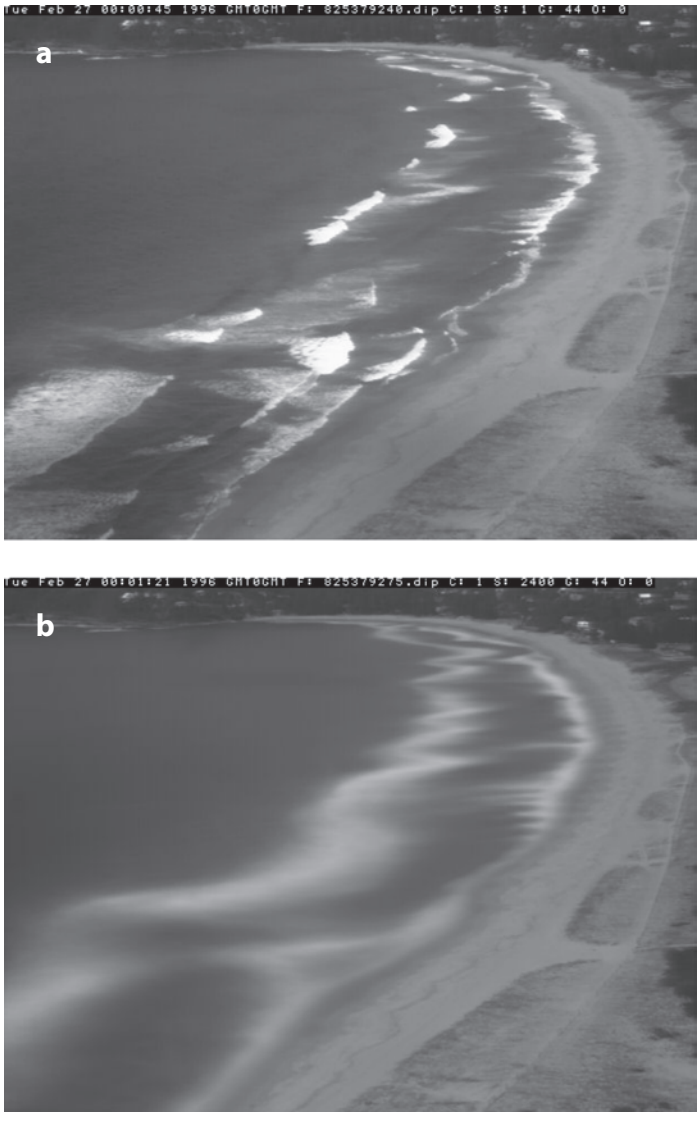

Figure 4

(*a*) Optical snapshot and (*b*) 10-min time exposure image at Palm Beach, Australia, approximately 30 km north of Sydney. The averaging process helps define regions of preferred breaking, which correspond to the shallow waters of offshore sand bars. The observed bar morphology is often surprisingly complex.

The introduction of roller physics also allowed an improved understanding of the relationship between widely used time exposure images and the wave dissipation that causes the breaking patterns. Aarninkhof & Ruessink (2004) introduced methods to partition time exposure optical intensity into the contributions from active breaking and those from residual foam left by breakers (e.g., see **Figure 7** in Section 3.4) and demonstrated the relationship between the adjusted intensities and modeled roller dissipation. This relationship is a component of the Beach Wizard algorithm for depth estimation (van Dongeren et al. 2008).

3.3. Bathymetry

Nearshore bathymetry is likely the variable that most limits the accuracy of numerical models. Bathymetry forms the bottom boundary for all flows, but under storm conditions it can undergo order-one changes over timescales as short as days (Sallenger et al. 1985). Moreover, nearshore wave dissipation and currents are quite sensitive to small changes in bathymetry, a sensitivity that can be exploited to improve sparse or inaccurate bathymetric estimates based on measurements of currents (Wilson et al. 2010).

The cost and logistical difficulties of tracking these bathymetric changes using traditional in situ surveying methods make this work expensive and uncommon. Survey update rates greater than once per year are rare and occur only at sites of special interest and investment. Thus, there is strong motivation for the development of remote sensing solutions.

For relatively clear water in which the bottom is directly visible, depth can be estimated by exploiting the wavelength-dependent attenuation of bottom-reflected light (deeper water appears blue because longer-wavelength red light preferentially attenuates) (Mobley 1994). Given knowledge of the optical properties of the water column and of the bottom reflectance, this sensitivity can be inverted to yield direct depth estimates (Mobley et al. 2005). Bottom characteristics in clear water can also be obtained by direct laser ranging (Irish & Lillycrop 1999). However, bottom visibility is not common on many beaches, especially at midlatitudes, where water clarity is usually reduced by fine grain sediments or surf zone microbubbles. Thus, alternate signatures must be exploited.

For cases of opaque water, bathymetry must be inferred from ocean surface signatures. Two such dependencies have been explored: wave dissipation and wave celerity. The depth dependence of surf zone wave dissipation is key to the use of 10-min time exposure images (**Figure 4*b***) in the Argus program. This simple method has proved to be an invaluable source of low-cost data on evolving sand bar morphologies (horizontal patterns) and has revealed the surprising complexity of these natural systems (e.g., Lippmann & Holman 1989, 1990; van Enckevort et al. 2004). Similar products have subsequently been demonstrated for marine radar observations (Ruessink et al. 2002, McNinch 2007).

The morphology patterns from time exposure images cannot be directly input into numerical models because they are not a direct measure of depth. However, because models can reasonably predict the average wave-breaking pattern over any bathymetry, observations of breaking can be compared with predicted patterns for various test bathymetries to find the one that is most consistent with observations. This approach was well documented and applied to a long-term data set by Aarninkhof et al. (2005), with good results through the surf zone (but limited insight for offshore waters).

An alternate approach exploits the dependence of wave speed, c (an observable quantity), on depth, h, as described by the wave dispersion relation (Dean & Dalrymple 1991)

$$c = \frac{L}{T} = \frac{gT}{2\pi} \tanh\left(\frac{2\pi h}{L}\right), \quad (1)$$

where L and T are the wave length and period, respectively, and g is the acceleration due to gravity. Thus, if the lengths and periods (and hence speeds) of waves can be observed, the depths can be estimated through a process called bathymetric inversion. This approach was first explored using airborne image sequences in World War II (Williams 1947), and while suitable for the idealized monochromatic waves of a laboratory, it was found to be much too sensitive to noise issues for natural random seas. Since then, considerable effort has gone into examining the limitations of the above model (e.g., Grilli 1998, Misra et al. 2003, Flampouris et al. 2011) and quantifying the inherent level of accuracy provided by remote sensing data in bathymetric inversion

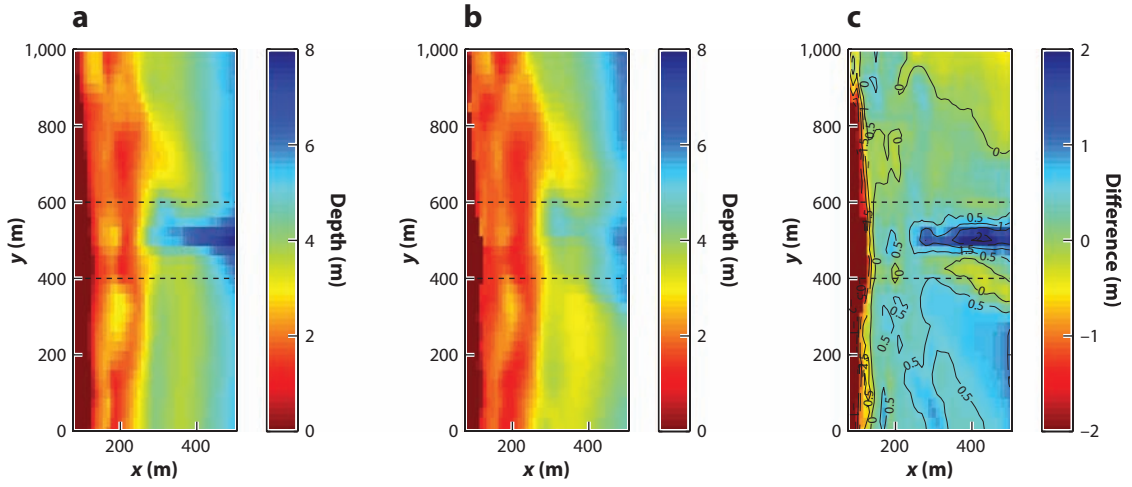

Figure 5

(*a*) Accurately measured bathymetry and (*b*) estimated bathymetry computed using the cBathy algorithm and optical observations, along with (*c*) the differences between the two. The central region, 400 m < *y* < 600 m, includes a pier that obscures the optical view and so is omitted from statistical analysis. Most errors are less than 0.5 m, and details of the sand bar (*x* < 250 m) are well rendered.

(Holland 2001, Catalan & Haller 2008, Plant et al. 2008). The Argus program has concentrated on steadily improving signal-processing methods, including frequency partitioning by Fourier analysis, empirical orthogonal function isolation of coherent wave components, and Kalman filtering to objectively span inevitable data gaps or poor results, finally yielding a fairly robust capability with bias and rms errors of 0.19 and 0.5 m, respectively, over a 1-km section of typical beach (cBathy algorithm; R.A. Holman, N.G. Plant & K.T. Holland, manuscript in review) (**Figure 5**). A separate effort, a program called Beach Wizard, combines Equation 1 with the dissipation-based method in a hybrid approach (van Dongeren et al. 2008).

3.4. Currents and Circulation

Bathymetry and offshore wave characteristics are sufficient inputs to run nearshore numerical models that can predict nearshore hydrodynamics and potentially bathymetric change. However, there is clear interest in the ability to directly measure currents and circulation in the nearshore both for its direct utility (for example, for estimating longshore sediment transport and shoreline change) and as confirmation of model performance.

Nearshore currents can be measured in several ways. The most direct is to track the trajectories of passive tracers (that is, anything whose movement is solely a result of water motion). IR imagery shows a wealth of small ephemeral thermal plume structures associated with nearshore turbulence (often left by breaking waves) whose lifetime is sufficient to use for PIV methods for mapping currents (**Figure 6**).

White foam left by breaking waves provides an alternate tracer that is strongly visible in optical images. Chickadel et al. (2003) developed a method for estimating longshore currents based on foam trajectories in a time-space image (e.g., **Figure 7**). Only the alongshore component of a current is estimated with this method, but cross-shore flow can also be estimated by requiring conservation of mass (alongshore divergences must be balanced by cross-shore convergences from which cross-shore flow can be integrated).

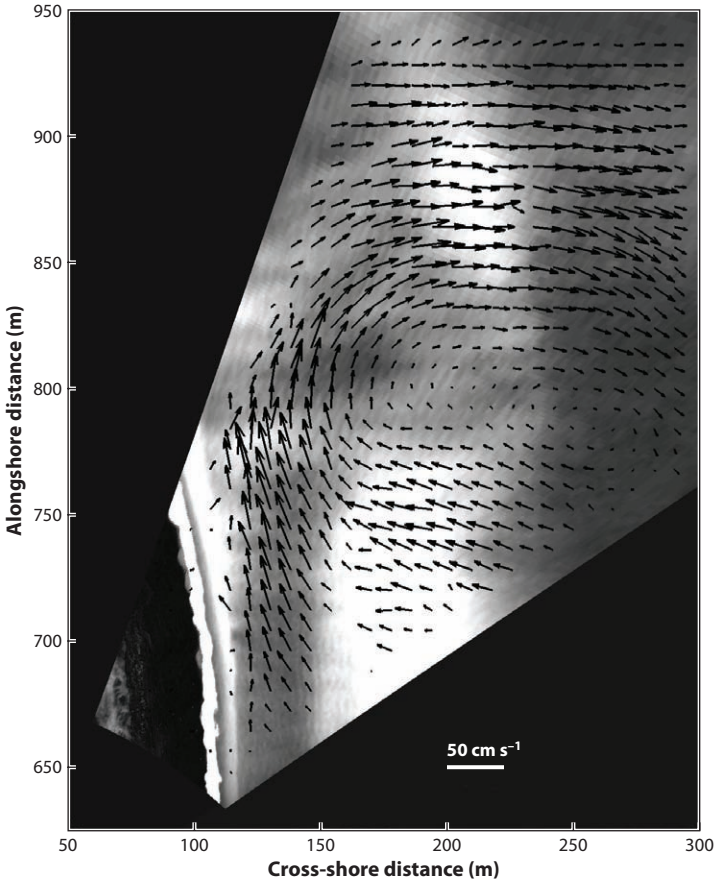

Figure 6

Example nearshore velocity field for Duck, North Carolina, estimated using particle image velocimetry (PIV) methods for tracking features in short-duration, time-averaged infrared images. The vectors indicate an eddy centered near $y = 800$ m with a rip current to the north. Image courtesy of Chris Chickadel, Applied Physics Laboratory, University of Washington.

Currents can also be estimated based on their Doppler shifting of the surface gravity wave field (e.g., Young et al. 1985, Senet et al. 2008), even in combination with bathymetric retrievals (e.g., Dugan et al. 2001b, Senet et al. 2008). However, these methods typically use Fourier transforms in space, which is an inherent limitation to resolution. Therefore, this method is typically not applied to surf zone currents.

4. THE FUTURE

Nearshore remote sensing is still a fairly new discipline, but one with a developing maturity. The sensors are quite capable, and the research needs focus partly on the continuing development of robust signal processing (which the human eye and brain do naturally).

The proliferation of new platforms such as small UAVs, especially at the hobby level, offers great promise but also challenges. Imagery from short-wingspan platforms is always jumpy. To stabilize aircraft flight, navigation systems filter these high-frequency shifts, and because the downlinked

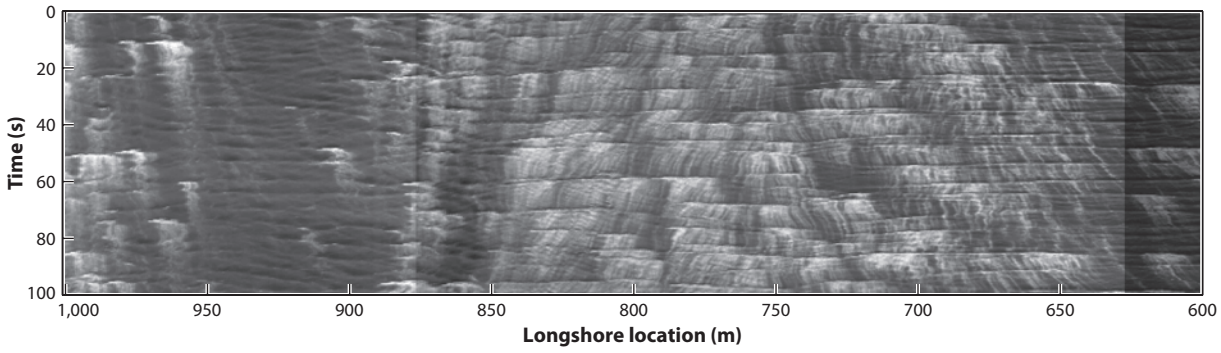

Figure 7

Time-space image of residual foam trajectories along a specific alongshore transect as the foam is carried by longshore currents. Horizontal features at roughly every 10 s in the vertical (time) axis correspond to the passage of waves past this cross-shore location, while the white oblique streaks correspond to residual foam left by breakers. Alongshore velocities can be estimated from the angle of these streaks—that is, how far they move across the horizontal (space) axis with increasing time down the vertical axis. The currents are therefore negative around $y = 950$ m (angling down to the right), positive around $y = 825$ m (angling down to the left), and then negative again around $y = 650$ m (again angling down to the right). Where currents converge (e.g., $y = 875$ m), there will be a corresponding rip current to balance that convergence.

navigation data are rarely in sync with instantaneous image shifts, simple georectification yields large errors. The lack of image-based stabilization for ocean-only scenes is currently a major hurdle.

There will clearly be improvements to sensors. At the low end, smartphones now provide high-quality imagery at low cost and weight, all controlled by a powerful operating system. At the other end of the spectrum, SAR and the associated complex processing algorithms continue to evolve. Interferometric SAR is a new capability that exploits the phase differences between two receiving antennae that are displaced in the along- or across-track direction to estimate mean currents or wave heights from imaged scenes. Both of these improvements are appropriate for airborne platforms.

Of the three sensor types considered here, optics has seen the most investigation as a nearshore sampling tool with multiple applications. Marine radar has only recently been adapted for nearshore use, and these efforts have focused more on the retrieval of wave parameters. Radar's day-night all-weather capabilities, large sampling range, and ease of spatial mapping make it a good tool for further investigation. IR sensors have only rarely been tested for nearshore applications but could provide valuable new signature opportunities and day-night imaging capability.

There is good reason to suspect that dissimilarities in the physics by which the three sensors interact with the nearshore ocean will allow interesting and powerful sensor fusion opportunities that would not be available from the simple addition of individual instrument capabilities. In addition, the sensors have complementary resolution and footprint characteristics that, in combination, can provide a more synoptic picture of the nearshore.

Remote sensing data analysis on its own is powerful, but less so than the assimilation of remote sensing data into numerical models of the nearshore. The situation is analogous to the assimilation of satellite-derived measurements into global circulation or tide models. Models represent the state of our knowledge of nearshore dynamics but require data inputs that are rarely well measured; remote sensing, in contrast, allows measurement of important quantities but with sampling noise that can be reduced by the implementation of dynamical consistency with models using data assimilation. The field of data assimilation of nearshore remote sensing data is new and promising.

5. CONCLUSIONS

The nearshore domain is characterized by rapid temporal changes, large variations over short spatial scales, and often-violent conditions. Traditional in situ sensors are poorly suited to sampling this world, but remote sensors offer potential solutions with temporal dwell, spatial reach, and a protected environment. The challenge is to develop methods to transform images from different sensors into geophysical data that can direct decisions or be incorporated into nearshore prediction models for full nearshore characterization.

Turning an imager into an instrument requires a good understanding of the geolocation of observed features and of the physics that links observations and geophysical quantities, as well as the development of robust algorithms to extract signals from often-noisy sources. The three most useful sensors sample at the optical, IR, and X-band radar wavelengths of the EM spectrum; from the data provided by these sensors, algorithms allow the estimation of subaqueous bathymetry, incident wave conditions, nearshore currents, and incident wave dissipation, the key variables required for nearshore characterization.

Some algorithms, such as the celerity-based estimation of bathymetry, are equally applicable to each of the sensors. Others, such as the estimation of wave height, exploit signatures specific to a particular sensor. Because each sensor interacts with the surface of the ocean differently, there exists nonredundant information that can potentially be exploited in more advanced algorithms. These fused data inputs, organized by the dynamical framework provided by models and data assimilation formalism, should yield powerful new information.

DISCLOSURE STATEMENT

The authors are not aware of any affiliations, memberships, funding, or financial holdings that might be perceived as affecting the objectivity of this review.

ACKNOWLEDGMENTS

Most of this work has developed over the careers of the authors and represents the combined efforts of many people. John Stanley has been responsible for the development and operation of the Argus program of optical remote sensing, which began at the Oregon State University Coastal Imaging Lab and has since spread worldwide, with the help of too many people to mention. Guillermo Diaz and David Honegger provided support on the marine radar section of this review, and Chris Chickadel and Andy Jessup helped greatly with the section on IR sensors. Tuba Özkan-Haller and Greg Wilson provided valuable insight into the netherworld of data assimilation. Adam Keen provided useful comments and editorial suggestions. Funding for the work has come from many sources over the years but principally from the Office of Naval Research Littoral Optics and Geosciences program (grant N00014-11-10393) and the Multidisciplinary University Research Initiative (grant N00014-10-1-0932), as well as from the Northwest Association of Networked Ocean Observing Systems (NANOOS).

LITERATURE CITED

Aagaard T, Holm J. 1989. Digitization of wave run-up using video records. *J. Coast. Res.* 5:547–51

Aarninkhof SGJ, Ruessink BG. 2004. Video observations and model predictions of depth-induced wave dissipation. *IEEE Trans. Geosci. Remote Sens.* 42:2612–22

Aarninkhof SGJ, Ruessink BG, Roelvink JA. 2005. Nearshore subtidal bathymetry from time-exposure images. *J. Geophys. Res.* 110:C06011

Aarninkhof SGJ, Turner IL, Dronkers TDT, Daljouw M, Nipius L. 2003. A video-based technique for mapping intertidal beach bathymetry. *Coast. Eng.* 49:275–89
Alexander P, Holman RA. 2004. Quantitative analysis of nearshore morphological variability based on video imaging. *Mar. Geol.* 208:101–11
Almar R, Cienfuegos RAR, Catalán PA, Michallet H, Castelle B, et al. 2012. A new breaking wave height direct estimator from video imagery. *Coast. Eng.* 61:42–48
Alpers WR, Ross DB, Rufenach CL. 1981. On the detectability of ocean surface waves by real and synthetic radar. *J. Geophys. Res.* 86:6481–98
Bass SJ, Hay AE. 1997. Ambient noise in the natural surf zone: wave-breaking frequencies. *IEEE J. Ocean. Eng.* 22:411–24
Bell PS. 1999. Shallow water bathymetry derived from an analysis of X-band marine radar images of waves. *Coast. Eng.* 37:513–27
Bell PS, Osler JC. 2011. Mapping bathymetry using X-band marine radar data recorded from a moving vessel. *Ocean Dyn.* 61:2141–56
Borge JCN, Reichert K, Dittmer J. 1999. Use of nautical radar as a wave monitoring instrument. *Coast. Eng.* 37:331–42
Branch R, Plant WJ, Gade M, Jessup AT. 2008. Relating microwave modulation to microbreaking observed in infrared imagery. *IEEE Geosci. Remote Sens. Lett.* 5:364–67
Bryan K, Coco G. 2010. Observations of nonlinear runup patterns on plane and rhythmic beach morphology. *J. Geophys. Res.* 115:C09017
Catalan PA, Haller MC. 2008. Remote sensing of breaking wave phase speed with application to nonlinear depth inversions. *Coast. Eng.* 55:93–111
Catalan PA, Haller MC, Holman RA, Plant WJ. 2011. Optical and microwave detection of wave breaking in the surf zone. *IEEE Trans. Geosci. Remote Sens.* 49:1879–93
Chickadel CC, Holman RA, Freilich MF. 2003. An optical technique for the measurement of longshore currents. *J. Geophys. Res.* 108:3364
Clarke LB, Werner BT. 2003. Synoptic imaging of nearshore bathymetry patterns. *J. Geophys. Res.* 108:3005
Coakley DB, Haldeman PM, Morgan DG, Nicolas KR, Penndorf DR, et al. 2001. Electromagnetic scattering from large steady breaking waves. *Exp. Fluids* 30:479–87
Curlander JC, McDonough RN. 1991. *Synthetic Aperture Radar: Systems and Signal Processing*. Wiley Ser. Remote Sens. New York: Wiley
Dankert H, Rosenthal W. 2004. Ocean surface determination from X-band radar-image sequences. *J. Geophys. Res.* 109:C04016
Dean RG, Dalrymple RA. 1991. *Water Wave Mechanics for Engineers and Scientists*. Adv. Ser. Ocean Eng. Vol. 2. Singapore: World Sci.
de Vries S, Hill DF, de Schipper MA, Stive MJF. 2011. Remote sensing of surf zone waves using stereo imaging. *Coast. Eng.* 58:239–50
Dugan JP, Fetzer GJ, Bowden J, Rarruggia GJ, Williams JZ, et al. 2001a. Airborne optical system for remote sensing of ocean waves. *J. Atmos. Ocean. Technol.* 18:1267–76
Dugan JP, Piotrowski CC, Williams JZ. 2001b. Water depth and surface current retrievals from airborne optical measurements of surface gravity wave dispersion. *J. Geophys. Res.* 106:16903–15
Duncan J. 1981. An experimental investigation of breaking waves produced by a towed hydrofoil. *Proc. R. Soc. Lond. A* 377:331–48
Elsayed MG, Takewaka S. 2008. Longshore migration of shoreline mega-cusps observed with X-band radar. *Coast. Eng.* 50:247–76
Feddersen F, Guza RT, Elgar S. 2004. Inverse modeling of one-dimensional setup and alongshore current in the nearshore. *J. Phys. Oceanogr.* 34:920–33
Flampouris S, Seemann J, Senet C, Ziemer F. 2011. The influence of the inverted sea wave theories on the derivation of coastal bathymetry. *IEEE Geosci. Remote Sens. Lett.* 8:436–40
Flampouris S, Ziemer F, Seemann J. 2008. Accuracy of bathymetric assessment by locally analyzing radar ocean wave imagery. *IEEE Trans. Geosci. Remote Sens.* 46:2906–13
Fuchs J, Regas D, Waseda T, Welch S, Tulin MP. 1999. Correlation of hydrodynamic features with LGA radar backscatter from breaking waves. *IEEE Trans. Geosci. Remote Sens.* 37:2442–60

Gommenginger CP, Ward NP, Fisher GJ, Robinson IS, Boxall SR. 2000. Quantitative microwave backscatter measurements from the ocean surface using digital marine radar images. *J. Atmos. Ocean. Technol.* 17:665–78

Grilli ST. 1998. Depth inversion in shallow water based on nonlinear properties of shoaling period waves. *Coast. Eng.* 35:185–209

Haller MC, Catalan PA. 2009. Remote sensing of wave roller lengths in the laboratory. *J. Geophys. Res.* 114:C07022

Haller MC, Lyzenga DR. 2003. Comparison of radar and video observations of shallow water breaking waves. *IEEE Trans. Geosci. Remote Sens.* 41:832–44

Hasan GMJ, Takewaka S. 2009. Wave run-up analyses under dissipative conditions using X-band radar. *Coast. Eng.* 51:177–204

Herbers THC, Elgar S, Guza RT. 1995. Infragravity-frequency (0.005–0.05 Hz) motions on the shelf. Part II: free waves. *J. Phys. Oceanogr.* 25:1063–79

Holland KT. 2001. Application of the linear dispersion relation with respect to depth inversion and remotely sensed imagery. *IEEE Trans. Geosci. Remote Sens.* 39:2060–72

Holland KT, Holman RA, Lippmann TC, Stanley J, Plant N. 1997. Practical use of video imagery in nearshore oceanographic field studies. *IEEE J. Ocean Eng.* 22:81–92

Holman RA, Stanley J. 2007. The history and technical capabilities of Argus. *Coast. Eng.* 54:477–91

Irish JL, Lillycrop WJ. 1999. Scanning laser mapping of the coastal zone: the SHOALS system. *ISPRS J. Photogramm. Remote Sens.* 54:123–29

Izquierdo P, Soares CG. 2005. Analysis of sea waves and wind from X-band radar. *Ocean Eng.* 32:1404–19

Ja SJ, West JC, Qiao HB, Duncan JH. 2001. Mechanisms of low-grazing-angle scattering from spilling breaker water waves. *Radio Sci.* 36:981–98

Jessup AT, Zappa C, Lowen M, Hesany V. 1997. Infrared remote sensing of breaking waves. *Nature* 385:52–55

Klemas V. 2011. Remote sensing techniques for studying coastal ecosystems. *J. Coast. Res.* 27:2–17

Kurapov AL, Egbert GD, Allen JS, Miller RN. 2007. Representer-based variational data assimilation in a nonlinear model of nearshore circulation. *J. Geophys. Res.* 112:C11019

Lewis BL, Olin ID. 1980. Experimental study and theoretical model of high-resolution radar backscatter from the sea. *Radio Sci.* 15:815–28

Lippmann TC, Holman RA. 1989. Quantification of sand bar morphology: a video technique based on wave dissipation. *J. Geophys. Res.* 94:995–1011

Lippmann TC, Holman RA. 1990. The spatial and temporal variability of sand bar morphology. *J. Geophys. Res.* 95:11575–90

Longuet-Higgins MS, Stewart RW. 1964. Radiation stresses in water waves; a physical discussion, with applications. *Deep-Sea Res.* 11:529–62

McGregor JA, Poulter EM, Smith MJ. 1998. *S* band Doppler radar measurement of bathymetry, wave energy fluxes, and dissipation across an offshore bar. *J. Geophys. Res.* 103:18779–89

McNinch JE. 2007. Bar and swash imaging radar (BASIR): a mobile X-band radar designed for mapping nearshore sand bars and swash-defined shorelines over large distances. *J. Coast. Res.* 23:59–74

Misra SK, Kennedy AB, Kirby JT. 2003. An approach to determining nearshore bathymetry using remotely sensed surface dynamics. *Coast. Eng.* 47:265–93

Mobley CD. 1994. *Light and Water: Radiative Transfer in Natural Waters*. San Diego: Academic

Mobley CD, Sundman LK, Davis CO, Downes TV, Leathers RA, et al. 2005. Interpretation of hyperspectral remote-sensing imagery via spectrum matching and look-up tables. *Appl. Opt.* 44:3576–92

Oltman-Shay J, Howd PA, Birkemeier WA. 1989. Shear instabilities of the mean longshore current 2. Field observations. *J. Geophys. Res.* 94:18031–42

Perkovic D, Lippmann TC, Frasier SJ. 2009. Longshore surface currents measured by Doppler radar and video PIV techniques. *IEEE Trans. Geosci. Remote Sens.* 47:2787–800

Plant NG, Holland KT, Haller MC. 2008. Ocean wavenumber estimation from wave-resolving time series imagery. *IEEE Trans. Geosci. Remote Sens.* 46:2644–58

Plant WJ. 1991. The variance of the normalized radar cross-section of the sea. *J. Geophys. Res.* 96:20643–54

Plant WJ, Keller WC. 1983. Parametric dependence of ocean wave-radar modulation transfer functions. *J. Geophys. Res.* 88:9747–56

Puleo JA, Farquharson G, Frasier SJ, Holland KT. 2003. Comparison of optical and radar measurements of surf and swash zone velocity fields. *J. Geophys. Res.* 108:3100

Rueben M, Holman RA, Cox D. 2011. Optical measurements of tsunami inundation through an urban waterfront modeled in a large-scale laboratory basin. *Coast. Eng.* 58:229–38

Ruessink BG, Bell PS, van Enckevort IMJ, Aarninkhof SGJ. 2002. Nearshore bar crest location quantified from time-averaged X-band radar images. *Coast. Eng.* 45:19–32

Ruessink BG, Miles JR, Feddersen F, Guza RT, Elgar S. 2001. Modeling the alongshore current on barred beaches. *J. Geophys. Res.* 106:22451–64

Sallenger AH, Holman RA, Birkemeier WA. 1985. Storm-induced response of a nearshore bar system. *Mar. Geol.* 64:237–58

Senet CM, Seemann J, Flampouris S, Ziemer F. 2008. Determination of bathymetric and current maps by the method DiSC based on the analysis of nautical X-band radar image sequences of the sea surface. *IEEE Trans. Geosci. Remote Sens.* 46:2267–79

Siddiqui MHK, Loewen MR, Richardson C, Asher WE, Jessup AT. 2001. Simultaneous particle image velocimetry and infrared imagery of microscale breaking waves. *Phys. Fluids* 13:1891–903

Stockdon HF, Holman RA. 2000. Estimation of wave phase speed and nearshore bathymetry from video imagery. *J. Geophys. Res.* 105:22015–33

Svendsen IA. 1984. Mass flux and undertow in a surf zone. *Coast. Eng.* 8:347–64

Thornton EB, Guza RT. 1982. Energy saturation and phase speeds measured on a natural beach. *J. Geophys. Res.* 87:9499–508

Thornton EB, Kim CS. 1993. Longshore current and wave height modulation at tidal frequency inside the surf zone. *J. Geophys. Res.* 98:16509–19

Valenzuela GR. 1968. Scattering of electromagnetic waves from a tilted slightly rough surface. *Radio Sci.* 3:1051–66

van Dongeren A, Plant NG, Cohen A, Roelvink D, Haller MC, Catalan P. 2008. Beach Wizard: nearshore bathymetry estimation through assimilation of model computations and remote observations. *Coast. Eng.* 55:1016–27

van Enckevort IMJ, Ruessink BG, Coco G, Suzuki K, Turner IL, et al. 2004. Observations of nearshore crescentic sandbars. *J. Geophys. Res.* 109:C06028

Walker RE. 1994. *Marine Light Field Statistics*. Wiley Ser. Pure Appl. Opt. New York: Wiley

Walton TL. 1993. Ocean City, Maryland, wave runup study. *J. Coast. Res.* 9:1–10

Watanabe Y, Mori N. 2008. Infrared measurements of surface renewal and subsurface vortices in nearshore breaking waves. *J. Geophys. Res.* 113:C07015

Williams WW. 1947. The determination of gradients on enemy-held beaches. *Geogr. J.* 109:76–93

Wilson GW, Özkan-Haller HT, Holman RA. 2010. Data assimilation and bathymetric inversion in a two-dimensional horizontal surf zone model. *J. Geophys. Res.* 115:C12057

Wright JW. 1968. A new model for sea clutter. *IEEE Trans. Antennas Propag.* 16:217–23

Young IR, Rosenthal W, Ziemer F. 1985. A three-dimensional analysis of marine radar images for the determination of ocean wave directionality and surface currents. *J. Geophys. Res.* 90:1049–59

Zappa CJ, Asher WE, Jessup AT. 2004. Microbreaking and the enhancement of air-water transfer velocity. *J. Geophys. Res.* 109:C08S16

Zappa CJ, Banner ML, Schultz H, Corrada-Emmanuel A, Wolff LB, Yalcin J. 2008. Retrieval of short ocean wave slope using polarimetric imaging. *Meas. Sci. Technol.* 19:055503

Annual Review of
Marine Science

Volume 5, 2013

Contents

Errata

An online log of corrections to *Annual Review of Marine Science* articles may be found at http://marine.annualreviews.org/errata.shtml